CHAPTER 10

INCREASED PRESENCE OF MONO-UNSATURATED FATTY ACIDS IN THE STRATUM CORNEUM OF HUMAN SKIN EQUIVALENTS

Jeroen van Smeden[1,*], Varsha S. Thakoersing[1,*], Aat Mulder[1], Rob Vreeken[2,3], Abdoelwaheb El Ghalbzouri[4], Joke A. Bouwstra[1]

[1] Division of Drug Delivery Technology, Leiden Academic Centre for Drug Research, Leiden University, Leiden, The Netherlands.
[2] Division of Analytical Biosciences, Leiden Academic Centre for Drug Research, Leiden University, Leiden, The Netherlands.
[3] Netherlands Metabolomics Centre, Leiden Academic Centre for Drug Research, Leiden University, Leiden, The Netherlands.
[4] Department of Dermatology, Leiden University Medical Center, Leiden, The Netherlands
*Both authors contributed equally to this work

Adapted from Journal of Investigative Dermatology. 2013. 133:59–67

Abstract

Previous results showed that our in-house human skin equivalents (HSEs) differ in their stratum corneum (SC) lipid organization compared with human SC. To elucidate the cause of the altered SC lipid organization in the HSEs, a recently developed liquid chromatography/mass spectrometry method was used to study the free fatty acid (FFA) and ceramide (CER) composition in detail. In addition, the SC lipid composition of the HSEs and human skin was examined quantitatively with high-performance thin layer chromatography. For the first time our results reveal that all our HSEs have an increased presence of mono-unsaturated FFAs compared with human SC. Moreover, the HSEs display the presence of CER species with a mono-unsaturated acyl chain, which are not detected in human SC. All HSEs also exhibit an altered expression of stearoyl-CoA desaturase, the enzyme that converts saturated FFAs to mono-unsaturated FFAs. Furthermore, the HSEs show the presence of twelve CER subclasses, similar to native human SC. However, the HSEs have increased levels of CERs [EOS] and [EOH] and CER species with short total carbon chains and a reduced FFA level compared with human SC. The presence of unsaturated lipid chains in HSE offers new opportunities to mimic the lipid properties of human SC more closely.

Introduction

Human skin equivalents (HSEs) provide a valuable tool to predict the permeation of substances through the skin[1-8] or to determine whether compounds are toxins, irritants, or sensitizers for the skin[9-12]. However, to obtain a reliable *in vitro – in vivo* correlation, it is a prerequisite that HSEs have a comparable skin barrier function as native human

skin. The main barrier for compound penetration is located in the lipid matrix of the stratum corneum (SC). This lipid matrix is mainly composed of cholesterol, free fatty acids (FFAs), and ceramides (CERs)[13,14]. The lipid composition determines the lipid organization in the SC and is therefore a key factor in determining the skin barrier function[15]. We have previously investigated the SC lipid organization of four of our in-house HSEs, namely the fibroblast derived matrix model (FDM), Leiden epidermal model (LEM), full-thickness collagen model (FTM), and full-thickness outgrowth (FTO). The LEM is a skin equivalent with only an epidermal compartment. The FDM is a model wherein fibroblasts produce their own extracellular matrix, whereas the FTM contains a dermal compartment that consists of rat tail collagen populated with human fibroblasts. In the FTO, a full thickness explant of native human skin is placed onto rat tail collagen and is allowed to expand and develop an epidermis. The skin models mimic many aspects of native human skin. However, they display some differences in their SC lipid organization. These differences may have an important role in their decreased permeability barrier compared with human SC[16,17]. As the lipid organization is dictated by the lipid composition, we determined the SC lipid composition of each HSE in detail to unravel the cause of their altered SC lipid organization. For this purpose, we quantitatively assessed the SC lipid composition of our in-house HSEs and native human SC with high-performance thin layer chromatography (HPTLC). Nine CER subclasses have been identified in native human SC using HPTLC[18], whereas twelve CER subclasses have been identified using a recently developed liquid chromatography/mass spectrometry (LC/MS) method[19]. In this study, we used LC/MS to determine whether all identified CER subclasses in native human SC are also present in the SC of our HSEs. In addition, detailed information on the chain length distribution and degree of saturation of each CER subclass and FFAs is provided and compared with the SC of native human skin. The expression pattern of several enzymes involved in the FFA and CER synthesis was also investigated to examine the biological cause of the altered SC lipid properties observed in the HSEs. This study has led to the identification of previously unreported targets that offer previously unreported opportunities to optimize the SC lipid properties of HSEs and mimic the barrier properties of native human skin even more closely.

Materials and Methods

Cell culture

Native human mammary or abdomen skin was obtained from adults undergoing surgery. Human skin left over from surgery was collected after written informed consent of the skin donors and institutional approval was obtained. The Declaration of Helsinki

Principles were followed when using human tissue. Normal human keratinocytes (NHKs) and human dermal fibroblasts were isolated as described before[20]. A detailed description of the required media is provided as supplementary information. NHKs used to create HSEs with only an epidermal compartment were cultured with the Dermalife K medium complete kit (Lifeline Cell Technology, Walkersville, MD) supplemented with 1% penicillin/streptomycin (Sigma, Zwijndrecht, The Netherlands) until they reached a maximum confluency of 80%. First and second passage NHKs were used to generate HSEs.

Dermal equivalents

Collagen-type I containing dermal equivalents: Collagen-type I containing dermal equivalents were generated as described earlier[20]. Details regarding the generation of the dermal equivalents are provided as Supplementary Information.

Fully human dermal equivalents: The dermal matrices for the FDMs were generated as decribed previously[21]. Details regarding the generation of the FDMs are provided as Supplementary Information.

Generation of HSEs

HSEs generated on collagen dermal equivalents referred to as FTM: One week after preparation of the collagen type I containing dermal equivalents $0.5 \cdot 10^6$ NHKs were seeded on top of each dermal equivalent. On the first two days, the HSEs were kept submerged in a medium consisting of DMEM and Ham's F12 (Invitrogen, Leek, The Netherlands) (3:1 v/v), 5% fetal bovine serum (FBS), 1% penicillin/streptomycin, 0.5 µM hydrocortisone, 1 µM isoproterenol and 0.5 µg/mL insulin. The following two days the HSEs were kept submerged in a similar medium, except that the FBS was reduced to 1% and 0.053 µM selenious acid (Johnson Matthey, Maastricht, The Netherlands), 10 mM L-serine (Sigma), 10 µM L-carnitine (Sigma), 1 µM α-tocopherol acetate (Sigma), 25 mM vitamin C and a lipid mixture of 3.5 µM arachidonic acid (Sigma), 30 µM linoleic acid (Sigma), 25 µM palmitic acid (Sigma) were added to the medium. Hereafter, the HSEs were lifted to the air/liquid interface and were nourished with a medium in which the FBS was omitted and the arachidonic acid concentration was increased to 7 µM. The medium was refreshed twice a week. The HSEs were harvested 16 days after seeding of the NHKs onto the dermal equivalents.

HSEs generated on fully human dermal equivalents referred to as FDM: Three weeks after seeding fibroblasts onto filter inserts $0.5 \cdot 10^6$ NHKs were seeded onto each dermal equivalent. The HSEs were further cultured as described for the FTMs.

HSEs generated on inert filter, referred to as Leiden epidermal model (LEM): LEMs were

generated as described previously[10] with slight modifications. $0.2 \cdot 10^6$ NHKs were seeded onto cell culture inserts (Corning tranwell cell culture inserts, membrane diameter 12 mm, pore size 0.4 µM, Corning Life Sciences, Amsterdam, The Netherlands). The cells were kept submerged for 2-3 days in Dermalife medium until confluency. On the following 2 days, the HSEs were kept submerged in CnT medium (CellnTec, Bern, Switzerland) supplemented according to the manufacturer's protocol and 1% penicillin/streptomycin solution, 1 µM α-tocopherol acetate, 25 µM vitamin C, and a lipid mixture of 7 µM arachidonic acid, 30 µM linoleic acid, and 25 µM palmitic acid. Hereafter, the cells were nourished with the same medium, but were grown at the air/liquid interface. The LEMs were harvested 16 days after seeding the NHKs onto the inserts.

Full thickness cultures (FTO): Full-thickness (4 mm) fat free punch biopsies obtained from abdomen or mammary skin were gently pushed into freshly generated collagen type 1 containing dermal equivalents. These HSEs were cultured similarly as described for the FTMs and FDMs, except that they were directly cultured at the air/liquid interface. The FTOs were grown for approximately 16 days.

Morphology and immunohistochemistry

Harvested HSEs were fixed in 4% (w/v) paraformaldehyde (Lommerse Pharma, Oss, The Netherlands), dehydrated and subsequently embedded in paraffin. 5 µm sections were cut and used for immunohistochemical staining of human SCD1 (100× dilution; Sigma), serine palmitoyltransferase (SPT; 400× dilution; Cayman Chemicals, Ann Arbor, MI) and CER synthase 3 (CERS3; 10× dilution; Atlas Antibodies, Stockholm, Sweden). Immunohistochemical stainings of the samples were performed with the R.T.U. Vectastain Elite ABC reagent kit (Vector Laboratories, Burlingame, CA). Details of the staining procedure are provided as Supplementary Information.

SC Isolation and lipid extraction

The SC of human abdomen or mammary skin was isolated as described previously[19]. The SC lipids were extracted according to the Bligh and Dyer procedure[22] with a series of chloroform/methanol mixtures (1:2, 1:1 and 2:1 v/v) for 1 hour each. The extracts were combined and treated with 0.25M KCl and water. The organic phase was collected and evaporated under a stream of nitrogen at 40°C. The obtained lipids were reconstituted in a suitable volume of chloroform/methanol (2:1 v/v) and stored at -20°C until use. To obtain enough lipids for quantification, the lipid extracts of 2-4 HSEs from the same experiment and donor were pooled. The SC lipid composition of the full-thickness explant could not be determined, because there was not enough material to extract.

HPTLC lipid quantification

The extracted SC lipids were quantified using HPTLC. The used solvent system to separate the lipids is provided elsewhere[23]. Co-chromatography of serial dilutions of standards was used to identify and quantify each lipid class. The standards consisted of cholesterol, palmitic acid, stearic acid, arachidic acid, tricosanoic acid, behenic acid, lignoceric acid, cerotic acid, and CERs [EOS], [NS], [NP], [EOH], and [AP]. CER nomenclature according to terminology of Motta *et al*.[24] and Masukawa *et al*.[25]. The CERs were provided by Cosmoferm (The Netherlands). All other compounds were purchased from Sigma (The Netherlands). The lipid fractions were visualized and quantified as described before[26]. For quantification, SC lipid samples of two donors were used of each HSE type and native human skin.

LC/MS lipid analysis

The SC lipid species in the pooled lipid extracts of the HSEs and native human skin were analyzed by LC/MS according to the method described elsewhere[19]. Briefly: an Alliance 2695 HPLC (Waters Corp., Milford, MA) was coupled to a TSQ Quantum MS (Thermo Finnigan, San Jose, CA) measuring in APCI mode. The total lipid concentration of all samples was around 1 mg/ml and the injection volume was set to 10 µl for the analysis of both CERs and fatty acids. CERs were separated using a PVA-Sil analytical column (5 µm particle size, 100 × 2.1 mm i.d. YMC, Kyoto, Japan) using a gradient mobile phase from heptane to heptane/isopropanol/ethanol at a flow rate of 0.8 mL/min. The scan range of the MS was set between 500-1200 amu, measuring in positive ion mode. FFAs were analyzed by introducing some adaptations to the setup used for CER analysis as will be described in detail elsewhere (van Smeden *et al*, submitted): separation was achieved using a LiChroCART Purospher STAR analytical column (55 × 2 mm i.d. Merck, Darmstadt, Germany) under a flow rate of 0.6 ml/min using a gradient system from acetonitril/H_2O to methanol/heptane. 1% $CHCl_3$ and 0.2% acetic acid (HAc) were added to both mobile phases as ionization enhancers. The ionization mode and scan range was altered to negative mode and 200-600 amu, respectively.

Results

HPTLC analysis reveals that the HSEs have a reduced SC FFA content compared with human skin

The SC lipids of the HSEs and human skin were extracted and quantified with HPTLC to determine whether the HSEs show differences in their lipid composition compared with human skin. Figure 1a shows that SC of the HSEs contains cholesterol, FFAs, and all CER

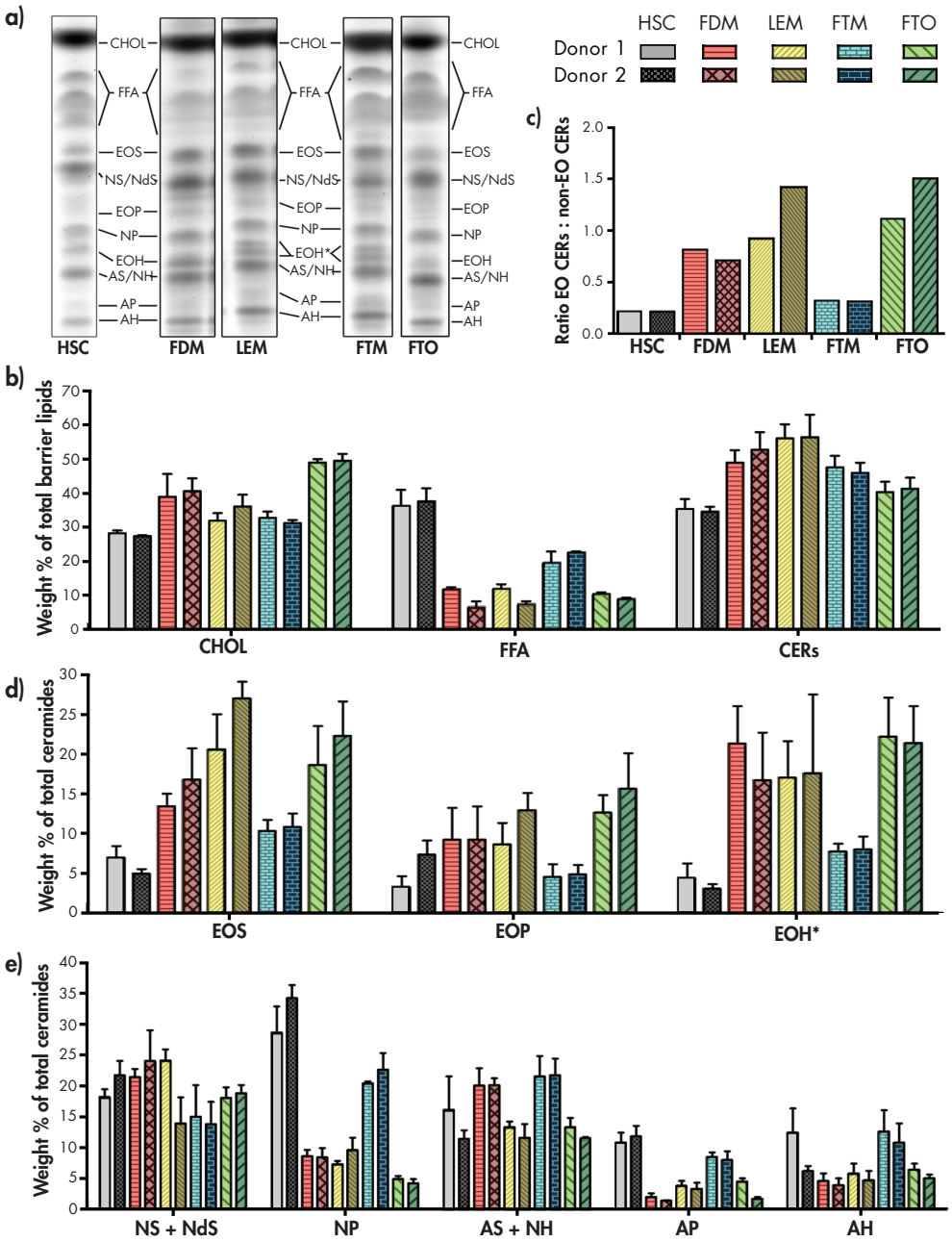

Figure 1: Stratum corneum barrier lipids content. *Barrier lipids of human stratum corneum (HSC), FDM, LEM, FTM, and FTO were fractionated and quantified by HPTLC and photo densitometry.* ***a****) Barrier lipid composition of human SC and HSEs.* ***b****) Relative level of each SC lipid class,* ***c****) ratio of acyl-CERs ([EO] CERs) and non-acyl-CERs (non-[EO] CER),* ***d****) relative level of acyl-CERs,* ***e****) relative level of* ***α****-hydroxy and non-hydroxy CERs. The data represents the sample mean ±SD of at least 3 analytical points. CHOL = cholesterol, FFA = free fatty acids, CERs = CERs, * unidentified lipid. CER nomenclature: A= **α**-hydroxy fatty acid, E = ester-linked fatty acid, N = non-hydroxy fatty acid, O = **ω**-hydroxy fatty acid, dS = dihydrosphingosine, H = 6-hydroxysphingosine, P = phytosphingosine, S = sphingosine.*

subclasses, which are also observed in human SC. In the LEM and FTM, an additional band of an unidentified lipid, with an R_f-value close to that of CER [EOH], can be observed. This unidentified lipid, which may represent an unidentified CER, was also occasionally observed in the FDM and FTO.

Figure 1b shows that human SC consists of approximately equal amounts of cholesterol, FFAs and CERs. All HSEs, however, show a different distribution of the SC barrier lipids (Figure 1b). The relative FFA content in the HSEs, especially in the FDM, LEM, and FTO, is much lower compared with human SC. The SC lipid quantification also indicates that the CER/cholesterol ratio (Supplementary Table 1) in the LEM is increased and reduced in FTO compared to human SC. This indicates that the relative CER and/or cholesterol levels in the SC of the LEM and FTO differ from the levels determined in human SC.

Most of the HSEs have an increased acyl-CER content compared with native human SC

In human SC twelve CER subclasses are identified. Each subclass is named according to its chemical structure[24,25]. In short, CERs with a sphingosine (S), phytosphingosine (P), 6-hydroxysphingosine (H), or dihydrosphingosine (dS) backbone are linked via an amide to a fatty acid chain, which can either be an esterified ω-hydroxy (EO), α-hydroxy (A), or non-hydroxy (N) fatty acid. Figure 1c shows the ratio between the total acyl-CERs ([EO] CERs) and the other CER classes (sum of all α-hydroxy + non-hydroxy CERs) in the HSEs and native human skin. This figure clearly shows that the total acyl-CERs level is much higher in the FDM, LEM, and FTO compared with native human skin. Focusing on the individual acyl-CER levels, it is evident that the FDM, LEM and FTO have a higher content of CERs [EOS] and [EOH]* compared with human SC. The difference in EOP level between FDM, LEM, FTO and human SC is somewhat smaller compared with the other acyl-CERs (Figure 1d). FTM has a small increase in CER [EOS] and [EOH]* level compared with human SC, while the [EOP] level is very similar (Figure 1d).

On the TLC plate, an unidentified lipid close to CER [EOH] is observed in the LEM and FTM (Figure 1a). In the LC/MS CER profiles of the HSEs, an unidentified group of lipids, which have a molecular weight similar to acyl-CERs, is also observed close to CER [EOH] (Figure 2b, indicated by **). This suggests that the lipid band on the TLC plate most likely represents an acyl-CER class. For this reason, the unidentified lipid was quantified together with CER [EOH] (the two bands together are represented as [EOH]*).

The comparison of the α-hydroxy and non-hydroxy CERs also shows some differences in the distribution of these CER subclasses between the HSEs and human SC (Figure 1e). CER [NP] is the most abundant CER in human SC. Compared with human SC, the CER [NP] content is reduced in the FTM and an even further reduction is observed in the FDM,

LEM, and FTO. In addition, the CER [AP] content in the FTM is close to the CER content in human SC, but reduced in the FDM, LEM and FTO. The relative content of CERs [NS] + [NdS], CERs [AS] + [NH], and CER [AH] are similar in the HSEs and human SC. CERs [NS] + [NdS], and [AS] + [NH] were grouped together for quantification, because they comigrate and therefore have a similar R_f-value when using HPTLC.

All twelve CER subclasses detected in human SC are also observed in the HSEs

LC/MS analysis of native human SC lipids shows the presence of at least twelve CER subclasses, as reported previously[19] (Figure 2a). In addition, within one CER subclass a large number of peaks are observed in the multi-mass chromatogram. Each peak represents a CER specie that has the same head group, but a different total carbon chain length and therefore a different molecular weight. In descending order, each specie has 14 mass units less, which represents a reduction in one CH_2-group compared with the previous specie. All twelve CER subclasses in human SC show a large variation in their total carbon chain length distribution. In human SC the acyl-CERs have a total chain length varying from 63 to 78 carbon atoms. The α-hydroxy and non-hydroxy CER subclasses have shorter total carbon chains, which range from 34 to 50 and 34 to 56 carbon atoms, respectively. In addition to the twelve identified CER subclasses, human SC also shows the presence of some unidentified lipid classes. These unidentified lipid classes also consist of several species, indicated by the variation in total carbon chain length. The molecular structure of these lipids remains to be elucidated. The CER subclasses present in the FDM, including the total chain length distribution of each subclass, is provided in the multi-mass chromatogram in Figure 2b. This figure shows that all twelve CER subclasses present in native human SC are also detected in FDM. The other HSEs show a very similar LC/MS profile as the FDM and also show the presence of all twelve CER subclasses (Supplementary Figure 1). Each CER subclass in the HSEs shows a wide variation in total chain length distribution, similar to native human SC. In the HSEs the acyl-CERs have a total carbon chain that varies between 64 and 78 carbon atoms, which is almost similar to the chain length distribution observed for native human SC. The α-hydroxy and non-hydroxy CER subclasses have a total carbon chain between 32 and 50 and 34 and 56 carbon atoms, respectively. When focusing in more detail on the LC/MS profiles of the HSEs and native human SC, some differences are observed. In the multi-mass chromatograms of the HSEs, a weak lipid band is located just below the stronger peaks of the CER species (Figure 2c), which is observed for all CER subclasses. These additional weak lipid bands always have a mass of two units less than that of stronger band of the CER specie above them (Figure 2c and d). This specific difference of two mass units suggests that the lipid band

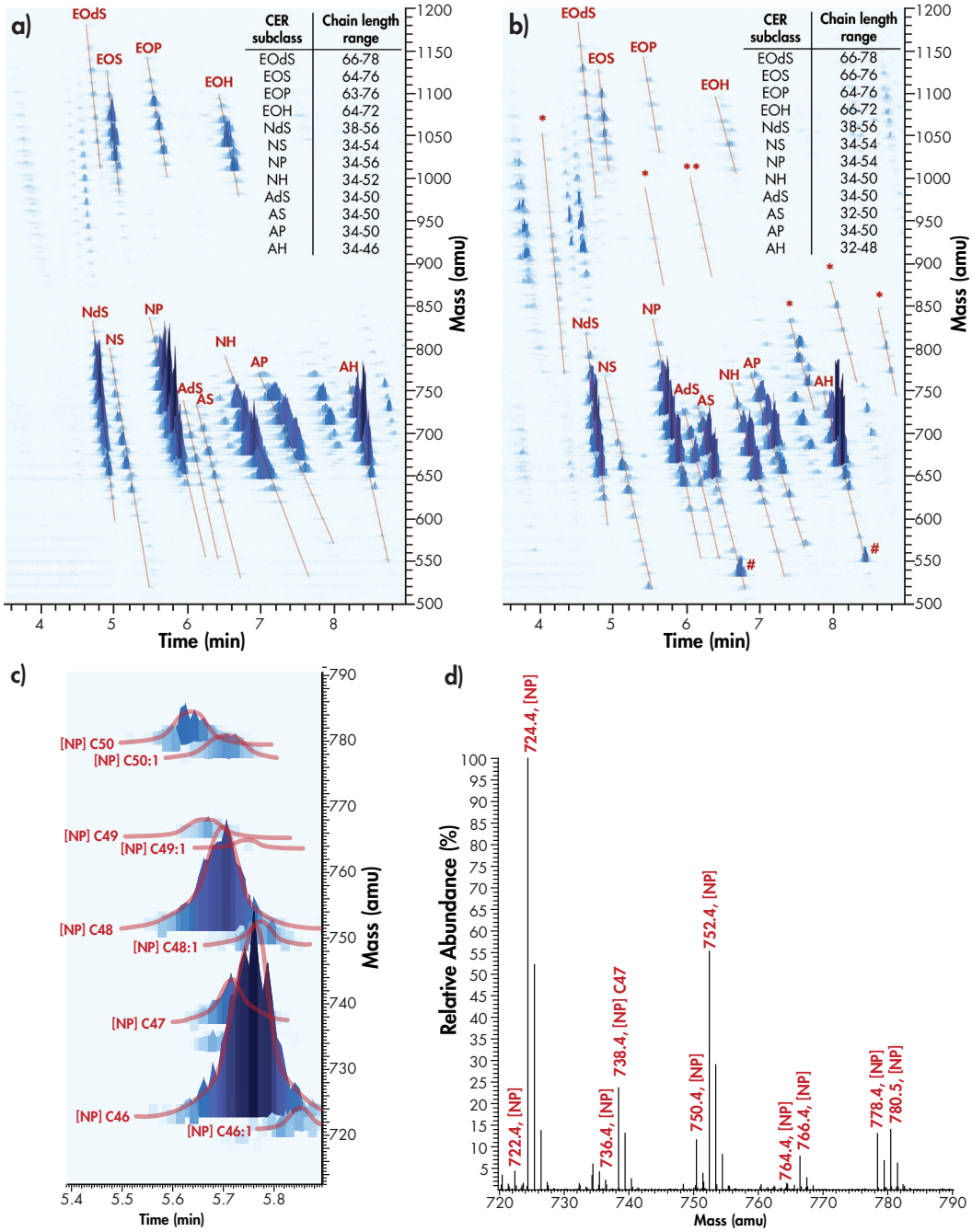

Figure 2: CER chain length distribution. *LC/MS chromatogram of CER subclasses in human SC* ***a)*** *and FDM* ***b)****. The retention time, mass and intensity of each peak are shown on the x-axis, y-axis and 'z'-axis, respectively. The total carbon chain length variation of each CER subclass is provided in the inset. CERs with a low total carbon chain length, which are present in lower quantities in human SC, are indicated by # in the chromatogram of FDM. Unidentified lipids only observed in the chromatogram of FDM are specified with *. The unidentified lipid quantified together with CER [EOH] using HPTLC is indicated by **. Examples of CER species containing a MUFA chain are shown in* ***c)****. The masses of CER species with a saturated or MUFA chain are shown in* ***d)****.*

represents a CER specie that contains a mono-unsaturated fatty acyl chain. The multi-mass chromatograms of the HSEs also show low molecular weight CER species that are not detected in human SC. Furthermore, some low molecular weight CER species, which have a mass below approximately 620 amu have a higher intensity in the multi-mass chromatograms of the HSEs compared with human skin. This is mainly observed for species of CERs [AS] and [AH], which have a total chain length of 34 carbon atoms (Figure 2b, indicated by #). The HSEs show the presence of several unidentified lipids, of which some are not present in the multi mass chromatogram of native human SC (Figure 2b, indicated by *).

HSEs show an increased presence of mono-unsaturated FFAs compared to native human SC

Figure 3 depicts the FFA chain length distribution and degree of saturation in human SC and FDM. The other HSEs showed a similar FFA composition as the FDM (Supplementary Figure 1). Human SC shows a FFA chain length distribution from C16:0 to C30:0. All HSEs contain FFAs with chain lengths varying from C16:0 to C28:0. This indicates that the HSEs are able to synthesize similar FFAs as native human skin. However, the FFA LC/MS profiles

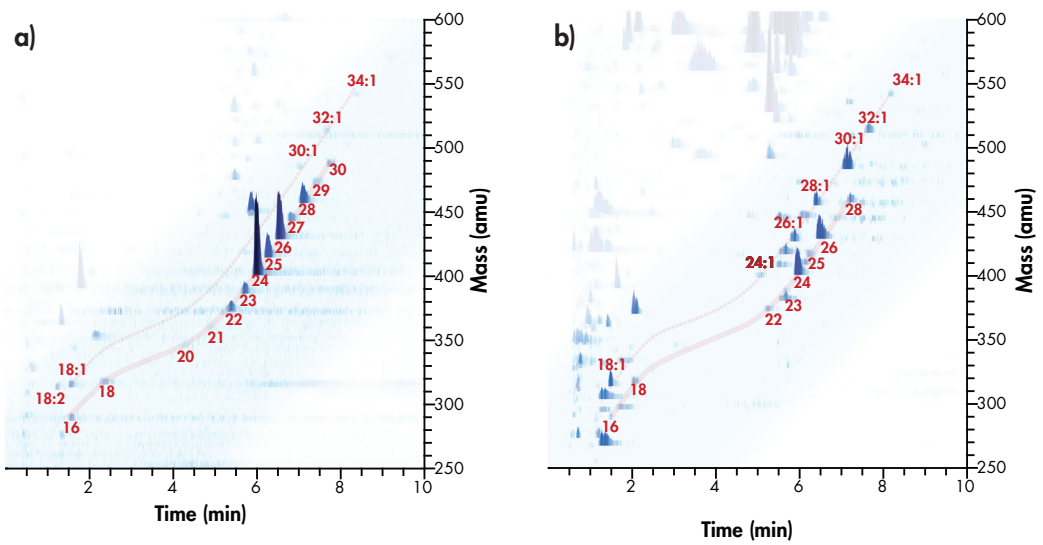

Figure 3: Fatty acid chain length distribution. *Three dimensional multi-mass LC/MS chromatogram of FFAs in native human SC* ***a****) and FDM* ***b****) are shown. The retention time is shown on the x-axis, the mass (in amu) is provided on the y-axis and the intensity of each peak is depicted on the 'z'-axis. In human SC the FFA chain length distribution varies from C16:0 to C30:0. The FDM has a very similar FFA chain length distribution as human SC, but shows an increase in MUFAs with chain lengths varying from C16:1 to C34:1. Additionally, the odd chain length FFAs show a lower intensity in the chromatogram of FDM compared to human SC.*

of all HSEs additionally show the presence of mono-unsaturated fatty acids (MUFAs), which are hardly detected in human SC. The MUFAs detected in the LC/MS profiles of the HSEs have a chain length varying from C16:1 up to C34:1. All HSEs also show a reduced level of FFAs with an odd carbon chain length compared with human SC.

The HSEs show an altered expression of stearoyl-CoA desaturase 1

To investigate the biological cause of the altered SC lipid organization of the HSEs, the expression pattern of some enzymes involved in the FFA and CER synthesis was examined. Stearoyl-CoA desaturase (SCD) is the rate-limiting enzyme that catalyzes the synthesis of MUFAs from saturated fatty acids[27,28]. In native human epidermis, SCD1 is only expressed in the basal layer (Figure 4). In all HSEs, the expression of SCD is observed in the basal layer, as well as in the differentiated layers of the viable epidermis (Figure 4). This indicates that the expression of SCD1 is altered in the HSEs compared with human skin.

The first step in CER synthesis is the coupling of serine to palmitic acid by serine palmitoyltransferase (SPT)[29]. In human skin, SPT expression is observed in the entire viable epidermis, showing both nucleic and cytoplasmic staining. No difference in expression pattern between human skin and the HSEs is observed (Figure 4). CER synthase 3 (CERS3) is one of the key enzymes involved in de novo CER synthesis pathway. CERS3 has a broad fatty acyl-coA preference and therefore *n*-acylates both long and very-long chain fatty acyl-CoAs to a sphingoid base. Among the six CERS members (CERS 1-6), the mRNA expression of CERS3 is found to be the highest in differentiated keratinocytes *in vitro*[30]. In addition, a recent publication by Jennemann *et al.*[31] demonstrated that CERS3 is responsible for the synthesis of very-long chain CERs in the skin. In human skin and in all HSEs, CERS3 is expressed in the entire viable epidermis (Figure 4). It should be noted that the expression of SCD, SPT, and CERS3 was weaker in the FTO samples compared with the other HSEs.

Discussion

In previous studies, we have investigated the SC lipid organization of four in-house HSEs and native human skin. These studies showed that our in-house HSEs have a mainly hexagonal packing[17], whereas human SC has the dense orthorhombic packing (a schematic representation of the SC lipid organization is depicted in Supplementary Figure 2). The presence of a hexagonal lipid organization has been correlated to a decreased skin barrier function as monitored by transepidermal water loss compared with the orthorhombic packing[32]. We examined the SC lipid composition of our HSEs in detail to verify the cause

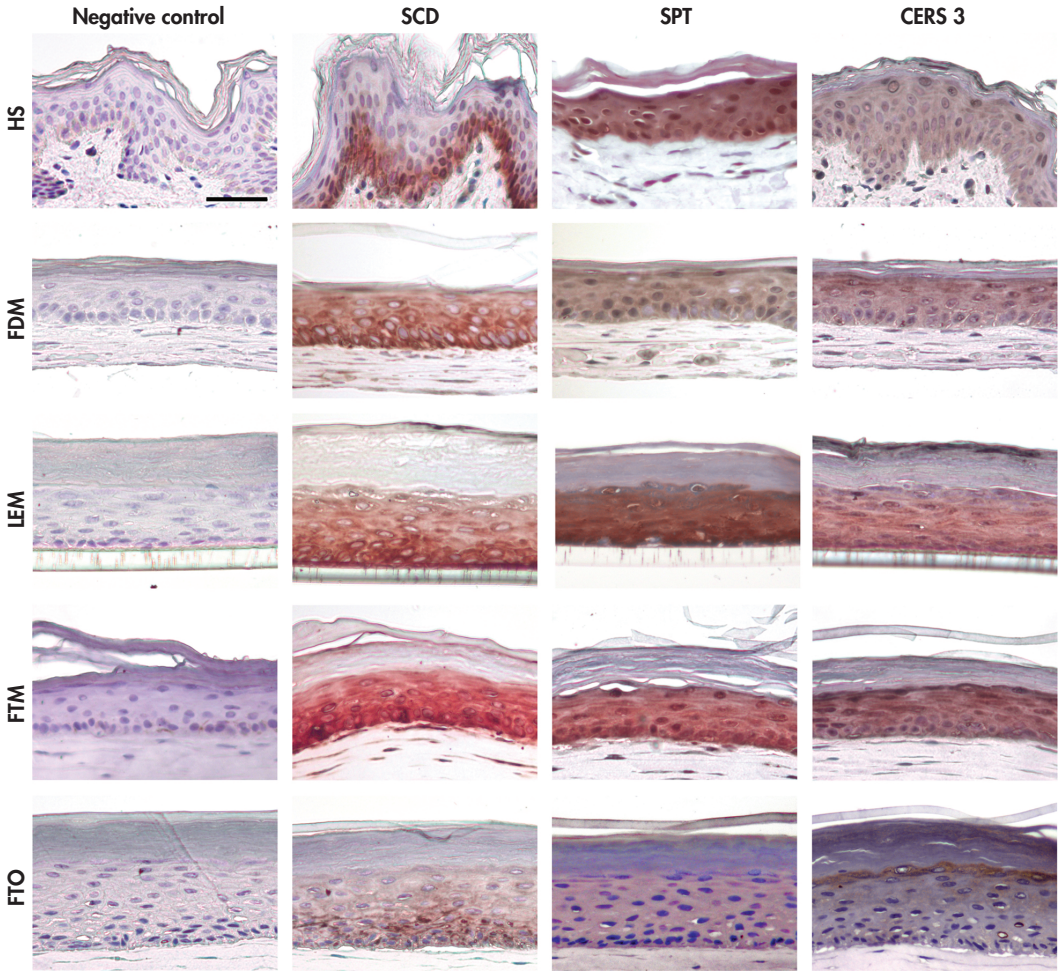

Figure 4: *Expression pattern of enzymes involved in free fatty acid desaturation and de novo CER synthesis. Immunohistochemical staining showing the expression pattern of stearoyl-CoA desaturase (SCD), serine palmitoyltransferase (SPT) and CER synthase 3 (CERS3) in human skin (HS), FDM, LEM, FTM and FTO. The negative control represents sections on which only the secondary antibody was applied. The micrographs were taken at a 20x magnification. Scale bar represents 50 μm.*

of their altered SC lipid properties and to determine how the latter can be optimized.

To our knowledge, it previously unreported that the SC of HSEs contain MUFAs, which may be a key factor for their altered SC lipid organization. The increase in MUFA content in the SC of HSEs coincides with the altered expression of SCD1 in the viable epidermis of the HSEs compared with human epidermis. It has been demonstrated that lipid mixtures containing an equimolar ratio of cholesterol, FFAs, and human CERs predominantly form an orthorhombic packing[33]. However, a reduction in FFAs or the addition of MUFAs in such

mixtures enhances the formation of a hexagonal lateral packing . This indicates that the reduction in FFA level and an increased presence of MUFAs contribute to the formation of the hexagonal packing in our HSEs and thus may be key factors in the observed increased benzocaine penetration across the SC of HSEs compared with native human skin. With respect to the lamellar phases, the HSEs show the predominant presence of the long periodicity phase (LPP)[17], whereas in human SC both the LPP and short periodicity phase (SPP) are formed[34]. All HSEs have an increased relative content of CERs [EOS] and [EOH]. As suggested in previous studies, these high acyl-CER levels may favor the formation of the LPP in HSEs[35], but does not make the HSEs more permeable.

We show that all twelve CER subclasses observed in native human SC are also present in the SC of all HSEs. This indicates that the keratinocytes in our HSEs retain their ability to synthesize all CER subclasses that are also present in human SC. This observation represents a big step forward in the characterization of the SC lipid properties of HSEs, considering that until now a maximum of nine CER subclasses were detected in HSEs, whereas in the commercial HSEs even those nine CER classes were not always present[18,36,37].
Masukawa *et al*. quantified the CER composition in native human SC using LC/MS[38]. The relative prevalence of each CER class determined in this study and the study of Masukawa *et al*. are very similar. In this study, five synthetic CERs are used for quantification of the SC lipids in the HSEs and native human SC. The use of several CER subclasses for quantification is very important, as the charring intensities of the CER subclasses differ considerably when equal amounts are sprayed on TLC plates (Supplementary Figure 3).
The different composition of CER subclasses in the FDM, LEM, and FTO compared with human skin is indicative of an altered CER subclass synthesis in these HSEs. The reason for this difference remains to be elucidated.

Our results demonstrate that the HSEs show a similar expression of CERS3 as human skin. The LC/MS multi mass chromatograms indeed show that the HSEs are able to synthesize CERs with a large variety in total carbon chain lengths, which are very similar to human skin. The expression of SCD1 in the proliferating and differentiating layers of the epidermis of the HSEs may result in an increased activity of SCD1 in the differentiated epidermal layers and thus an increased intracellular content of MUFAs in the keratinocytes. Because of the increase in intracellular MUFA content, the CERS enzymes, including CERS3, *n*-acylate both MUFAs and saturated FFAs to the sphingoid bases. The observation that an increase in MUFA content in the SC is accompanied by the presence of CER species with a mono-unsaturated fatty acyl chain suggests that fatty acids present in the SC and the fatty acyl chains of CERs have a common source or synthetic pathway.

The results of this study indicate that the SC lipid properties of the HSEs can be improved

by increasing the FFA content in the SC. The culture medium used to generate the HSEs is supplemented with FFAs. Optimization of FFA supplementation to the culture medium may lead to SC FFA levels that more closely resemble the SC FFA level of native human skin. At present it is unclear why the HSEs show an altered expression of SCD1 compared to human skin. It is possible that the culture conditions or certain media components which are known to affect SCD expression or activity, such as insulin, glucose and fatty acids[27,39] lead to an increased MUFA level in HSEs. However, it remains to be established whether increased expression of SCD1 in the suprabasal layers of the HSEs is truly associated with an increased activity of SCD1 compared with native human epidermis. If this appears to be true, the SC lipid properties can additionally be improved by reducing SCD1 activity and thereby the MUFA level in the SC of HSEs. SCD1 activity in the HSEs may therefore be reduced by using, e.g., SCD inhibitors[27,40] in the culture medium. Studies performed by Miyazaki *et al* 41 have demonstrated that SCD-deficient mice show skin permeability barrier defects, such as an insufficient lipid deposition in the SC due to the presence of immature lamellar bodies with a reduced lipid content, and a reduction in acyl-CER content. The reduction in SCD1 activity should therefore be performed with care to prevent different types of SC barrier defects in HSEs that may occur by a too severe suppression of SCD1 activity. Optimization of the FFA content in the SC of HSEs will be the subject of future studies.

Acknowledgements

The authors thank Maria Ponec for helpful suggestions during the meetings. We like to thank Evonik (Essen, Germany) for providing the CERs. This research is supported by the Dutch Technology Foundation STW, which is part of the Netherlands Organisation for Scientific Research (NWO), and which is partly funded by the Ministry of Economic Affairs.

References

1 Ackermann K, Borgia SL, Korting HC *et al.* The Phenion full-thickness skin model for percutaneous absorption testing. *Skin Pharmacol Physiol* 2010; 23: 105-12.

2 Asbill C, Kim N, El-Kattan A *et al.* Evaluation of a human bio-engineered skin equivalent for drug permeation studies. *Pharm Res* 2000; 17: 1092-7.

3 Batheja P, Song Y, Wertz P *et al.* Effects of growth conditions on the barrier properties of a human skin equivalent. *Pharm Res* 2009; 26: 1689-700.

4 Marjukka Suhonen T, Pasonen-Seppanen S, Kirjavainen M *et al.* Epidermal cell culture model derived from rat keratinocytes with permeability characteristics comparable to human cadaver skin. *Eur J Pharm Sci* 2003; 20: 107-13.

5 Netzlaff F, Kaca M, Bock U *et al.* Permeability of the reconstructed human epidermis model Episkin in comparison to various human skin preparations. *Eur J Pharm Biopharm* 2007; 66: 127-34.

6 Schafer-Korting M, Bock U, Diembeck W *et al.* The use of reconstructed human epidermis for skin absorption testing: Results of the validation study. *Altern Lab Anim* 2008; 36: 161-87.

7 Schmook FP, Meingassner JG, Billich A. Comparison of human skin or epidermis models with human and animal skin in in-vitro percutaneous absorption. *Int J Pharm* 2001; 215: 51-6.

8 Zghoul N, Fuchs R, Lehr CM *et al.* Reconstructed skin equivalents for assessing percutaneous drug absorption from pharmaceutical formulations. *Altex* 2001; 18: 103-6.

9 Alepee N, Tornier C, Robert C *et al.* A catch-up validation study on reconstructed human epidermis (SkinEthic RHE) for full replacement of the Draize skin irritation test. *Toxicol In Vitro* 2009; 24: 257-66.

10 El Ghalbzouri A, Siamari R, Willemze R *et al.* Leiden reconstructed human epidermal model as a tool for the evaluation of the skin corrosion and irritation potential according to the ECVAM guidelines. *Toxicol In Vitro* 2008; 22: 1311-20.

11 Gibbs S. In vitro irritation models and immune reactions. *Skin Pharmacol Physiol* 2009; 22: 103-13.

12 Netzlaff F, Lehr CM, Wertz PW *et al.* The human epidermis models EpiSkin, SkinEthic and EpiDerm: an evaluation of morphology and their suitability for testing phototoxicity, irritancy, corrosivity, and substance transport. *Eur J Pharm Biopharm* 2005; 60: 167-78.

13 Feingold KR. The outer frontier: the importance of lipid metabolism in the skin. J Lipid Res 2009; 50 Suppl: S417-22.

14 Wertz PW. Lipids and barrier function of the skin. *Acta Derm Venereol Suppl (Stockh)* 2000; 208: 7-11.

15 Bouwstra JA, Ponec M. The skin barrier in healthy and diseased state. Biochim Biophys Acta 2006; 1758: 2080-95.

16 Thakoersing VS, Gooris GS, Mulder A *et al.* Unraveling barrier properties of three different in-house human skin equivalents. *Tissue engineering. Part C, Methods* 2012; 18: 1-11.

17 Thakoersing VS, Gooris G, Mulder AA *et al.* Unravelling Barrier Properties of Three Different In-House Human Skin Equivalents. *Tissue Eng Part C Methods* 2011.

18 Ponec M, Weerheim A, Lankhorst P *et al.* New acylCER in native and reconstructed epidermis. *J Invest Dermatol* 2003; 120: 581-8.

19 Van Smeden J, Hoppel L, van der Heijden R *et al.* LC/MS analysis of stratum corneum lipids: CER profiling and discovery. *J Lipid Res* 2011; 52: 1211-21.

20 Bouwstra JA, Groenink HW, Kempenaar JA *et al.* Water distribution and natural moisturizer factor content in human skin equivalents are regulated by environmental relative humidity. *J Invest Dermatol* 2008; 128: 378-88.

21 El Ghalbzouri A, Commandeur S, Rietveld MH *et al.* Replacement of animal-derived collagen matrix by human fibroblast-derived dermal matrix for human skin equivalent products. *Biomaterials* 2009; 30: 71-8.

22 Bligh EG, Dyer WJ. A rapid method of total lipid extraction and purification. Can J Biochem Physiol 1959; 37: 911-7.

23 Thakoersing VS, Ponec M, Bouwstra JA. Generation of human skin equivalents under submerged conditions-mimicking the in utero environment. *Tissue Eng Part A* 2010; 16: 1433-41.

24 Motta S, Monti M, Sesana S *et al.* CER composition of the psoriatic scale. Biochim Biophys Acta 1993; 1182: 147-51.

25 Masukawa Y, Narita H, Shimizu E *et al.* Characterization of overall CER species in human stratum corneum. *J Lipid Res* 2008; 49: 1466-76.

26 Rissmann R, Groenink HW, Weerheim AM *et al.* New insights into ultrastructure, lipid composition and organization of vernix caseosa. *J Invest Dermatol* 2006; 126: 1823-33.

27 Ntambi JM, Miyazaki M, Dobrzyn A. Regulation of stearoyl-CoA desaturase expression. Lipids 2004; 39: 1061-5.

28 Zhang L, Ge L, Parimoo S *et al.* Human stearoyl-CoA desaturase: alternative transcripts generated from a single gene by usage of tandem polyadenylation sites. *Biochem J* 1999; 340 (Pt 1): 255-64.

29 Gault CR, Obeid LM, Hannun YA. An overview of sphingolipid metabolism: from synthesis to breakdown. *Adv Exp Med Biol* 2010; 688: 1-23.

30 Mizutani Y, Mitsutake S, Tsuji K *et al.* CER biosynthesis in keratinocyte and its role in skin function. *Biochimie* 2009; 91: 784-90.

31 Jennemann R, Rabionet M, Gorgas K *et al.* Loss of CER synthase 3 causes lethal skin barrier disruption. *Hum Mol Genet* 2012; 21: 586-608.

32 Damien F, Boncheva M. The extent of orthorhombic lipid phases in the stratum corneum determines the barrier efficiency of human skin in vivo. *J Invest Dermatol* 2010; 130: 611-4.

33 Bouwstra J, Pilgram G, Gooris G *et al.* New aspects of the skin barrier organization. *Skin Pharmacol Appl Skin Physiol* 2001; 14 *Suppl 1:* 52-62.

34 Bouwstra JA, Gooris GS, van der Spek JA *et al.* Structural investigations of human stratum corneum by small-angle X-ray scattering. *J Invest Dermatol* 1991; 97: 1005-12.

35 De Jager M, Gooris G, Ponec M *et al.* AcylCER head group architecture affects lipid organization in synthetic CER

mixtures. *J Invest Dermatol* 2004; 123: 911-6.

36 Ponec M, Boelsma E, Gibbs S *et al.* Characterization of reconstructed skin models. *Skin Pharmacol Appl Skin Physiol* 2002; 15 *Suppl 1:* 4-17.

37 Ponec M, Weerheim A, Kempenaar J *et al.* The formation of competent barrier lipids in reconstructed human epidermis requires the presence of vitamin C. *J Invest Dermatol* 1997; 109: 348-55.

38 Masukawa Y, Narita H, Sato H *et al.* Comprehensive quantification of CER species in human stratum corneum. *J Lipid Res* 2009; 50: 1708-19.

39 Mauvoisin D, Mounier C. Hormonal and nutritional regulation of SCD1 gene expression. *Biochimie* 2011; 93: 78-86.

40 Liu G. Stearoyl-CoA desaturase inhibitors: update on patented compounds. *Expert Opin Ther Pat* 2009; 19: 1169-91.

41 Miyazaki M, Dobrzyn A, Elias PM *et al.* Stearoyl-CoA desaturase-2 gene expression is required for lipid synthesis during early skin and liver development. *Proc Natl Acad Sci U S A* 2005; 102: 12501-6.

Supplementary information – Materials & Methods

Cell culture

Human dermal fibroblasts were cultured in DMEM (Invitrogen, Leek, The Netherlands) supplemented with 5% fetal bovine serum (FBS; Hyclone, Logan, UT) and 1% penicillin/streptomycin (Sigma). Normal human keratinocytes were grown in medium consisting of DMEM and Hams's F12 (Invitrogen, Leek , The Netherlands) (3:1 v/v), 5% FBS, 1% penicillin/streptomycin, 1 μM hydrocortisone (Sigma), 1 μM isoproterenol (Sigma) and 0.5 μg/mL insulin (Sigma).

Dermal equivalents

Collagen-type I containing dermal equivalents: a 1 mg/mL collagen, isolated form rat tails, solution was obtained by mixing a 4 mg/mL collagen solution in 0.1% acetic acid with Hank's buffered salt solution (Invitrogen, Leek, The Netherlands), 0.1% acetic acid, 1M NaOH and FBS (Hyclone, Logan, UT) on ice. One mL of this mixture was pipetted into a filter insert (Corning transwell cell culture inserts, membrane diameter 24 mm, pore size 3 μm, Corning Life Sciences, Amsterdam, The Netherlands) and polymerized for 15 minutes at 37°C. Hereafter, a 2 mg/mL collagen layer was prepared as described, with the addition of fibroblasts to the FBS solution (final fibroblast cell density of $0.4 \cdot 10^5$ cells/mL collagen solution). Three mL of this fibroblast-populated collagen mixture was pipetted onto the previous collagen layer and polymerized as described. The dermal equivalents were transferred to a 6-well deep-well plate (Organogensis, Canton, MA) and cultured under submerged conditions in medium consisting of Dulbecco's Modified Eagle medium (DMEM; Invitrogen, Leek, The Netherlands), 5% FBS, 1% penicillin/streptomycin (Sigma) and fresh supplementation of 45 mM vitamin C (Sigma). The medium was refreshed twice a week.

Fully human dermal equivalents: $0.4 \cdot 10^6$ fibroblasts were seeded onto filter inserts (Corning Transwell culture inserts, membrane diameter 24 mm, pore size 0.4 μm; Corning Life Sciences, Amsterdam, The Netherlands) and were nourished with a similar medium described for the collagen type I containing dermal equivalents. The fibroblast were allowed to generate their own extracellular matrix for 3 weeks. The medium was refreshed twice a week.

Morphology and immunohistochemistry

The paraffin sections were deparaffinized and rehydrated through xylene and graded

ethanol series and finally washed with PBS. Antigen retrieval was performed by immersion in sodium citrate buffer (pH 6) for 30 minutes close to the boiling point. After cooling the sections were blocked with normal horse serum for 20 min, followed by incubation with the primary antibody (diluted to the appropriate concentration in 1% BSA in PBS) overnight at 4°C. After washing with PBS the sections were incubated with the secondary antibody for 30 minutes, washed again and incubated with ABC reagent for 30 minutes. The sections were consecutively washed with PBS, 0.1 M sodium acetate buffer and incubated for 30 minutes in amino-ethylcarbazole (Sigma) dissolved in N,N-dimethylformamide (1 g/250 mL) (Sigma) supplemented with 0.1% hydrogen peroxide and finally with water. Counterstaining was performed with haematoxylin. Incubation with normal horse serum, secondary antibody and ABC reagent were performed with the R.T.U. Vectastain Elite ABC reagent kit (Vector Laboratories, Burlingame, CA).

Supplementary information – Figures and Table

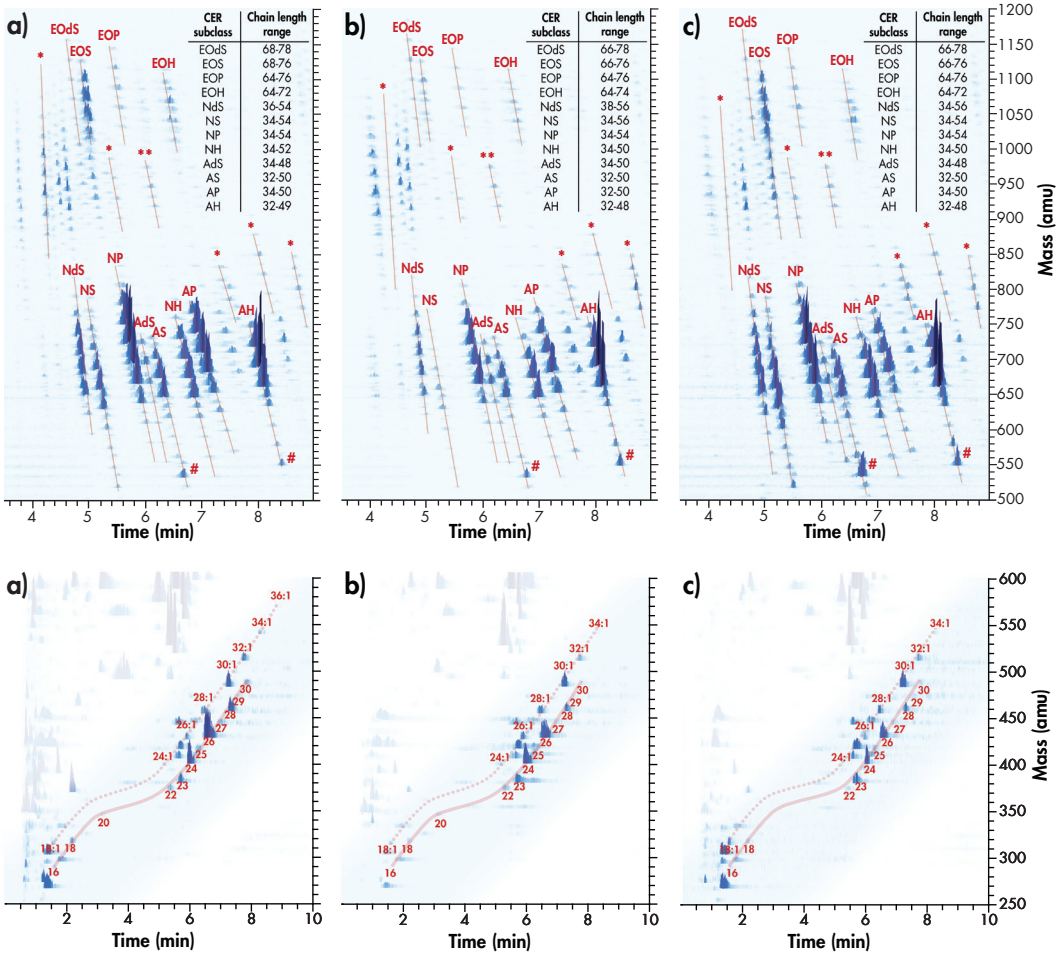

Supplementary Figure 1: *Ceramide and FFA chain length distribution in LEM, FTM and FTO. Three dimensional multi-mass LC/MS chromatogram of ceramide subclasses in LEM* ***a****), FTM* ***b****) and FTO* ***c****). The retention time is shown on the x-axis, the mass is provided on the y-axis and the intensity of each peak is depicted on the 'z'-axis. The total carbon chain length variation of each ceramide subclass is indicated in the inset. Ceramides with a low total carbon chain length which are present in lower quantities in human SC are indicated by #. Unidentified lipids observed in the chromatogram of the LEM, FTM and FTO which are not observed in human SC are specified with *. The unidentified lipid quantified together with ceramide [EOH] using HPTLC is indicated by **. The FFA chain length distribution and degree of saturation of LEM, FTM and FTO are shown in* ***d****),* ***e****) and* ***f****), respectively.*

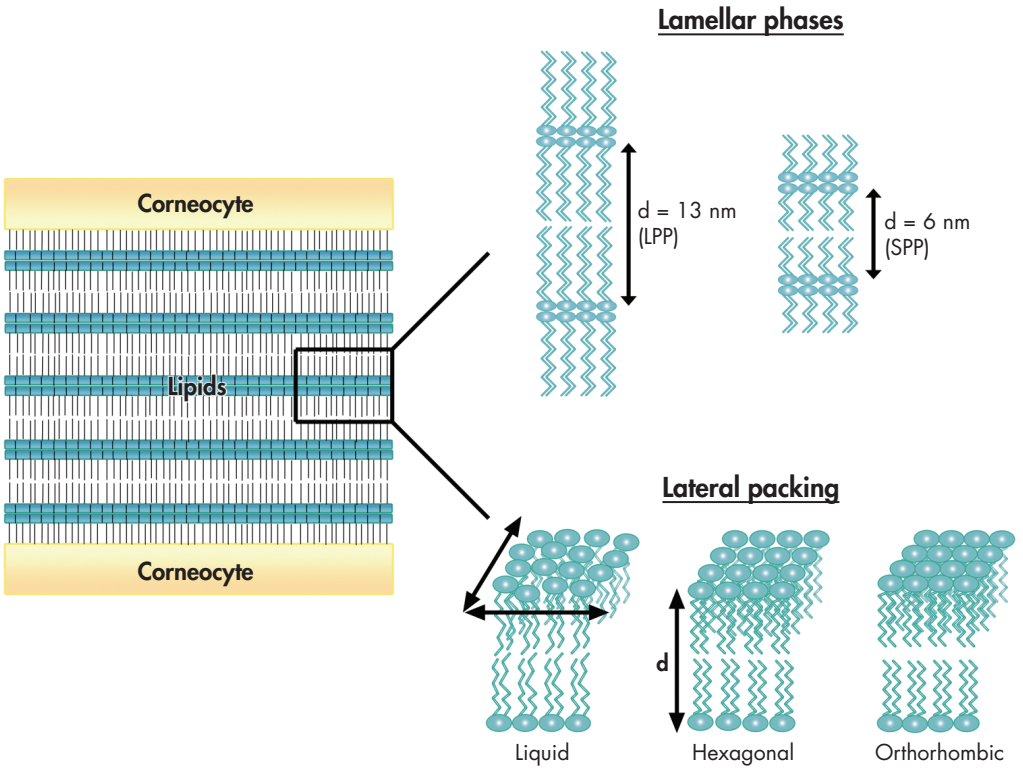

Supplementary Figure 2: Stratum corneum lipid organization. *In human SC the lamellar phases refer to the stack of lipid layers (i.e. lipid lamellae) between the corneocytes. The distance over which one lipid layer is repeated is referred to as the repeat distance* ***d****). In human SC the lipid lamellae have a repeat distance of approximately 13 or 6 nm, the long and short periodicity phase (LPP and SPP), respectively. The lateral packing discloses the density of the lipids within the lipid lamellae. The orthorhombic packing has the highest lipid density and the liquid packing the lowest. In human SC the lipids are arranged in the orthorhombic packing, although some lipid domains also form the hexagonal or liquid packing.*

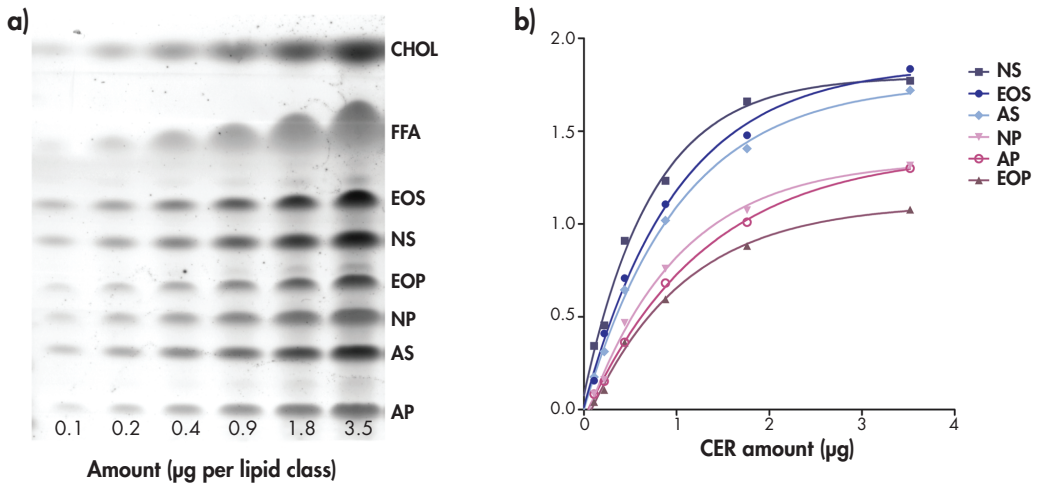

Supplementary Figure 3: Charring differences of ceramide standards. *Figure* ***a****) shows the charring intensities of the lipid standards used for the quantification of the* SC *lipid composition. The lipid standard contains equal weight amounts of each standard. The charring intensity of each spot was determined by densitometry and plotted against the amount sprayed to construct a calibration curve* ***b****).*

Supplementary Table 1

Skin source	Ceramide/Cholesterol ratio	
HSC	Donor 1	1.3
	Donor 2	1.3
FDM	Donor 1	1.3
	Donor 2	1.3
LEM	Donor 1	1.8
	Donor 2	1.6
FTM	Donor 1	1.5
	Donor 2	1.5
FTO	Donor 1	0.8
	Donor 2	0.8